Simplified Vent Sizing Equations for Emergency Relief Requirements in Reactors and Storage Vessels

Simplified vent sizing equations for emergency relief requirements in reaction kettles and storage vessels are obtained from analytical consideration. Venting modes include homogeneous-vessel venting, all-vapor venting, and all-liquid venting; energy sources due to runaway chemical reactions and external heating are treated separately. The resulting equations have been shown via numerical examples to yield good agreement with detailed computer simulations, both in terms of temperature and pressure histories during venting and in vent size predictions. These equations are generally applicable over a wide range of overpressure situations and reduce to the correct limit at no overpressure. The relative merit of allowing for overpressure in various venting modes can be demonstrated using these equations. Because of their simple forms, requiring only pertinent physical property and thermal data, these equations readily lend themselves to quick but accurate vent sizing predictions.

J. C. Leung
Fauske & Associates, Inc.
Burr Ridge, IL 60521

Introduction

Detailed analysis of reactor venting subjected to runaway reactions invariably involves the use of a large computer code which often requires in its input a very large thermophysical property data base as well as a kinetic model for the runaway reaction (Booth et al., 1980; Huff, 1984b; Grolmes and Leung, 1985). The acquisition of such data can be time-consuming and very costly. The purpose of this paper is to develop analytical vent sizing equations in simple closed-form expressions for runaway reactors undergoing various venting modes, namely, homogeneous-vessel venting, all-liquid venting, and all-vapor venting. As such, these equations are applicable to a major class of runaway reactions where the exotherm is tempered by evaporative cooling of the volatile components (Huff, 1982). In addition, similar equations are presented for storage vessels under external heating such as fire exposure situations.

In the past several methods of calculation have been proposed for sizing emergency relief systems (ERS). One common, but frequently nonconservative method is based on vapor venting alone (Diss et al., 1961). As noted by several early observers (Boyle, 1967; Harmon and Martin, 1970; Huff, 1973) the most realistic case should be based on the release of a vapor-liquid mixture, with two-phase discharge in the relief system. Boyle developed the first theoretically design method based on liquid discharge and defined the required vent area as that size which would empty the reactor before the pressure could rise above some allowable overpressure for a given vessel. This can be represented mathematically as

$$A = \frac{m_o}{G\Delta t_p} \tag{1}$$

where the emptying time Δt_p is based on the pressure history obtained from adiabatic runaway computation or data in a sealed sytem, Figure 1. However, Boyle's assumption of nonflashing liquid discharge often leads to unrealistic high flow, since in reality the discharge liquid will flash and subsequently attain choking at the exit piping. Hence, the use of flashing choked flow in Eq. 1 has been proposed subsequently by Huff (1973), Duxbury (1980), and Fauske (1984a,b). Fauske (1984b) approximated the required venting time by

$$\Delta t_p = \frac{\Delta T}{(dT/dt)_s} \tag{2}$$

where $(dT/dt)_s$ is the temperature rise rate (commonly known

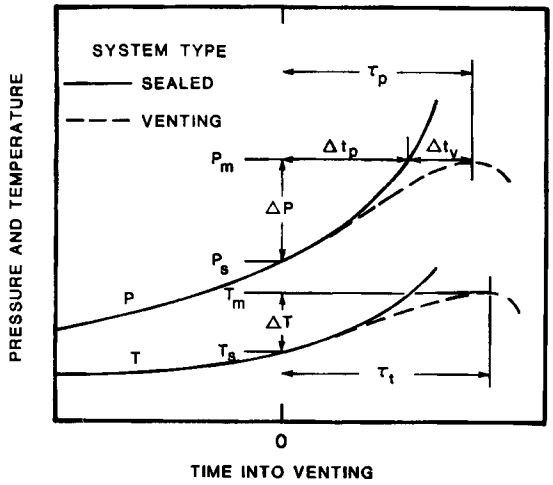

Figure 1. Characteristic time in vented and nonvented runaways.
(Adapted from Huff, 1982).

as self-heat rate in runaway reactions) at the set pressure, and ΔT is the temperature rise corresponding to the overpressure ΔP. This venting time is often longer than Boyle's definition since it is based on a linear extrapolation and not on an average self-heat rate during the overpressure period. By proposing a simple formula for the flashing choked flow G (as will be discussed later) and utilizing Eqs. 1 and 2, Fauske obtained the following simple expression

$$A = \frac{m_o}{\Delta P}\left(\frac{C_p}{T_s}\right)^{1/2}\left(\frac{dT}{dt}\right)_s \tag{3}$$

Furthermore, by considering the case of 20% absolute overpressure (i.e., 0.2 P_s abs.) and taking a typical liquid specific heat of 2,100 J/kg · K (0.5 cal/g°C) for most organics, Fauske (1984c) constructed a generalized nomograph based on saturated water relationship.

The most comprehensive of the analytical methods to date is that of Huff (1977, 1982). The required vent rate W or GA in kg/s is calculated for temperature turnaround conditions taking into consideration the reduction in vessel contents during venting as well as the additional time required to generate the heat for vapor formation during venting, shown as Δt_v in Figure 1. By approximating the turnaround time in pressure τ_p by the turnaround time in temperature τ_t, Huff obtained the homogeneous-vessel venting result, casting it in terms of a relief vent rate requirement as

$$W = GA = (m_o/\tau_t) - (\beta/2\tau_t^2)[(1 + 4m_o\tau_t/\beta)^{1/2} - 1] \tag{4}$$

where,

$$\beta = \frac{h_{fg}V}{q_m v_{fg}}; \quad \tau_t = \Delta t_p + \frac{h_{fg}}{q_m}(x_m - x_o);$$

$$x_m = \frac{V/m_m - v_f}{v_{fg}}; \quad m_m = m_o - W\tau_t \tag{5}$$

Iteration is required to solve the above equations for W and τ_t since the latter is not readily obtainable.

In the present paper, analytical closed-form expressions for both τ_t and W are obtained for the homogeneous-vessel venting case as well as limiting cases such as all-vapor venting and all-liquid venting. For the three examples considered, the current method yields vent sizing results comparable to those of the computer simulations. Utilizing these equations, the relative merit of allowing for overpressure in the three venting modes can be demonstrated. In the case of all-vapor venting, there is no merit in allowing for overpressure. In the other two venting modes, substantial reduction in vent area is obtained by allowing for small overpressure. The relatively less reduction in the external heating situation also can be explained by the current approach. In general, the most stringent relief requirement is due to all-liquid venting. Since this venting mode is unlikely for a top-venting ERS design, the homogeneous-vessel behavior offers the next most stringent requirement and is therefore the recommended design approach for this configuration. Sizing based on all-vapor venting is both unrealistic and unsafe.

Governing Equations

Governing equations for relief vent rate requirement can be obtained by first considering the macroscopic energy and mass balance on the vessel as shown in Figure 2. For the bulk of the fluid in the vessel, the unsteady-state energy balance, Eq. 15.1-3 of Bird et al. (1960), becomes

$$\frac{d}{dt}(\rho V u) = Q - W\left(u_1 + \frac{P}{\rho_1}\right) \tag{6}$$

in which Q is the sum of all heat transfer and reaction energy rates and subscript 1 denotes the location at the vent line entry point. In writing this equation, both the kinetic and potential energies of the fluid have been neglected. The unsteady-state mass balance takes the form

$$\frac{d}{dt}(\rho V) = -W \tag{7}$$

Combination of the mass and energy balances then gives

$$\rho V\frac{du}{dt} = Q - W\left(u_1 - u + \frac{P}{\rho_1}\right) \tag{8}$$

This equation can be rewritten as follows by recalling $\rho V = m$, $\rho = 1/v$, $v = v_f + xv_{fg}$, $u = u_f + xu_{fg}$, and $h = u + Pv$:

$$m\left(\frac{du_f}{dT} + x\frac{du_{fg}}{dT}\right)\frac{dT}{dt} = Q - W[(x_1 - x)u_{fg} + Pv_1] - mu_{fg}\frac{dx}{dt} \tag{9}$$

This is essentially Huff's (1977) result for the general energy equation. For the case of ideal gas and incompressible liquid, Huff showed that the lefthand side of Eq. 9 reduces to

$$m\left\{x(C_{pg} - R) + (1 - x)\left[C_{pf} - T\left(\frac{dv_f}{dT}\right)\left(\frac{dP}{dT}\right)\right]\right\}\frac{dT}{dt}$$

(More correctly this term should reduce to $m[x(C_{pg} - R) +$

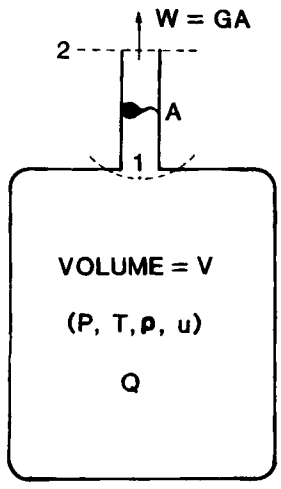

Figure 2. Reference vessel for model development.

$(1 - x)C_{pf}]dT/dt$ since the incompressible liquid assumption implies v_f = constant; $C_{pf} = C_{vf}$; see discussion, Bird et al., 1960, p. 459). However, for most practical situations (far from critical point and with vessel nearly full) it is accurate enough to represent this bulk sensible heat accumulation term by the liquid phase portion alone, i.e., $mC_{vf}(dT/dt)$. This representation is consistent with the unsteady-state energy equation discussed in reactor design textbooks (Smith, 1970, p. 109). The mass balance in Eq. 7 can be expanded to give

$$m\frac{dv}{dt} = Wv \tag{10}$$

while noting $dV/dt = 0$. By further assuming constant phasic specific volume properties, Eq. 10 reduces to

$$\frac{dx}{dt} = \frac{Wv}{mv_{fg}} \tag{11}$$

which simply states that the change in vessel quality is related to the net increase in vapor weight fraction as a result of relief discharge. Utilizing this result in the general energy equation, Eq. 9, we arrive at the final useful form of the energy equation

$$mC_{vf}\frac{dT}{dt} = Q - Wh_{fg}\left(x_1 + \frac{v_f}{v_{fg}}\right) \tag{12}$$

Hereafter, the subscript f in C_{vf} is dropped for convenience.

The energy input term Q can be further broken down into two categories: one due to the total reaction energy release and the other due to external heating such as fire exposure or jacket heating. The former is dependent on the instantaneous reacting mass, composition, and temperature; typically one can write $Q_{rxn} = mq$ where q is the reaction heat release rate per unit mass. The latter is treated as constant for simplicity during relief, i.e., $Q_{ext} = Q_T$, a constant. The solution schemes and final equations are noticeably different according to whether Q is mass-dependent or not. Finally, the second term on the righthand side of Eq. 12 represents the net evaporative cooling effect. It is given by the volumetric discharge rate $W(v_f + x_1 v_{fg})$, divided by v_{fg} to yield the net vapor production rate within the vessel, and multiplied by the latent heat to give the energy removal rate via evaporative cooling.

Homogeneous-Vessel Venting with Runaway Reaction

We treat here the particular case of zero disengagement of liquid and vapor within the vessel, the so-called uniform-froth or homogeneous-vessel venting case. For this case $x_1 = x$, and $v_1 = v = V/m$; the energy equation, Eq. 12, then takes the form

$$mC_v\frac{dT}{dt} = mq - GA\frac{V}{m}\frac{h_{fg}}{v_{fg}} \tag{13}$$

(We shall use W and GA interchangeably throughout the development.) This equation together with the mass balance, Eq. 7, can be integrated if one makes the following simplifications:

1. Mass flux G varies little during the overpressure transient.
2. Reaction energy per unit mass q is treated as constant and takes on an appropriate average value.
3. Properties such as C_v, h_{fg}, and v_{fg} are assumed constant.

Assumption 1 results in decoupling the two differential equations, while the other two assumptions permit integral solution. Note that if q takes on the familiar Arrhenius form or an exponential form such as $q = Ke^{aT}$, this will lead to a nonlinear equation that can only be solved numerically. All three assumptions do not result in any severe loss in accuracy when compared to a more detailed transient computer calculation as will be demonstrated.

To facilitate the integration, the following dimensionless variables are defined:

$$T^* \equiv (T - T_s)/(T_m - T_s) \tag{14a}$$

$$t^* \equiv t/t_e \tag{14b}$$

where

$$t_e = \frac{m_o}{GA} \tag{14c}$$

(Here t_e is similar to Δt_p in Eq. 1, but a simpler nomenclature is preferred here.) From Eq. 7 with constant G, integration yields the instantaneous mass given by

$$m = m_o - GAt = m_o(1 - t^*) \tag{15}$$

After substituting Eq. 15 into Eq. 13 and defining yet another dimensionless variable $N \equiv C_v(T_m - T_s)/h_{fg}$, the resulting integration takes the form

$$\int_o^{T^*} N dT^* = \int_o^{t^*} t_e\frac{q}{h_{fg}}dt^* - \frac{V}{m_o v_{fg}}\int_o^{t^*}\frac{dt^*}{(1 - t^*)^2} \tag{16}$$

Expanding and evaluating at both limits yields the following equation for the temperature history as a function of time:

$$NT^* = \frac{qt_e}{h_{fg}}t^* - \frac{V}{m_o v_{fg}}\frac{t^*}{(1 - t^*)} \tag{17a}$$

or in dimensional form:

$$T = T_s + \frac{qt}{C_v} - \frac{Vh_{fg}}{m_o C_v v_{fg}}\left(\frac{t}{t_e - t}\right) \tag{17b}$$

The next step is to solve for the dimensionless turnaround time τ^* by differentiating Eq. 17a with respect to time and setting dT^*/dt^* to zero,

$$\tau^* = 1 - \left(\frac{V}{m_o v_{fg}}\frac{h_{fg}}{qt_e}\right)^{1/2} \tag{18a}$$

where $\tau^* = \tau/t_e$, or in dimensional form

$$\tau = t_e - \left(\frac{Vh_{fg}}{m_o v_{fg}}\frac{t_e}{q}\right)^{1/2} \tag{18b}$$

Equation 18b says that the turnaround time τ is always less than the emptying time as long as evaporative cooling is present. Substitution of Eq. 18a into Eq. 17a then yields an expression relating the temperature at turnaround ($T^* = 1.0$) as a function of emptying time,

$$\frac{qt_e}{h_{fg}} = \left[\left(\frac{V}{m_o v_{fg}}\right)^{1/2} + N^{1/2}\right]^2 \tag{19}$$

Utilizing the definitions for t_e and N, Eq. 19 can be cast explicitly in terms of relief vent rate as,

$$W = GA = \frac{m_o q}{\left[\left(\frac{V}{m_o}\frac{h_{fg}}{v_{fg}}\right)^{1/2} + (C_v \Delta T)^{1/2}\right]^2} \tag{20}$$

where ΔT is simply the "overtemperature," $T_m - T_s$. Note that for the case of no overpressure ($\Delta P = 0$, $\Delta T = 0$), Eq. 20 reduces to the correct limiting form

$$A_o = \frac{m_o q_s v_{fg}}{G v h_{fg}} \tag{21}$$

which can be obtained by simply equating the two terms on the righthand side of the energy equation, Eq. 13. A number of possible ways of evaluating q are:

1. $q = q_m$ (at turnaround)
2. $q = \frac{1}{2}(q_s + q_m)$ (arithmetic average)
3. $q = (q_s q_m)^{1/2}$ (geometric average)
4. $q = (q_m - q_s)/\ln(q_m/q_s)$ (log mean)

where q_s and q_m are, respectively, the energy release rate at the set temperature and the turnaround temperature. The simple arithmetic average is recommended here, and applying Eq. 13 to a sealed vessel, q can be related to the temperature rise rate in a nonvented system, i.e.,

$$q = \frac{1}{2} C_v \left[\left(\frac{dT}{dt}\right)_s + \left(\frac{dT}{dt}\right)_m\right] \tag{22}$$

This expression will hence be used throughout the examples to be discussed later.

Finally, the corresponding overpressure can be estimated via the vapor pressure relation. For example, experimental P-T data can be easily correlated using the typical two- or three-constant Antoine equation. The underlying assumption is that either the system would exhibit pseudo one-component behavior such that during the short venting period, the effect on pressure as a result of composition change is negligible (constant volatility) or the system volatility is decreasing with venting.

All-vapor and All-liquid Venting with Runaway Reaction

All-vapor venting and all-liquid venting represent, respectively, top and bottom venting modes for vessels exhibiting complete vapor-liquid phase separation or disengagement. Due to the similarity in the final equations, they are discussed together here without detailing the mathematical steps; however, the solution technique remains the same as in the homogeneous-venting case. The energy equation, Eq. 12, now becomes

$$mC_v \frac{dT}{dt} = mq - GAv_i \frac{h_{fg}}{v_{fg}} \tag{23}$$

where $v_i = v_g$ for all-vapor venting and $v_i = v_f$ for all-liquid venting. Upon integration, the temperature history is given by:

$$T = T_s + \frac{qt}{C_v} + \frac{h_{fg}}{C_v}\frac{v_i}{v_{fg}}\ln\left(1 - \frac{t}{t_e}\right) \tag{24}$$

and the time at turnaround is

$$\tau = t_e - \left(\frac{v_i}{v_{fg}}\frac{h_{fg}}{q}\right) \tag{25}$$

The relief vent rate, GA, in this case is given implicitly by the following

$$T_m - T_s = \frac{m_o q}{GAC_v}\left(1 - \frac{A}{A_o}\right) + \frac{v_i h_{fg}}{v_{fg} C_v}\ln\left(\frac{A}{A_o}\right) \tag{26}$$

where,

$$A_o = \frac{m_o q_s v_{fg}}{G v_i h_{fg}} \tag{27}$$

For the no-overpressure case, Eq. 26 reduces to the correct limit with $A = A_o$.

Homogeneous-Vessel Venting with External Heating

Here we are limited to nonreacting systems subjected to constant energy input, Q_T. In this case, Eq. 12 becomes

$$mC_v \frac{dT}{dt} = Q_T - GA\frac{V}{m}\frac{h_{fg}}{v_{fg}} \tag{28}$$

Again using treatment similar to that in the runaway reaction system, this equation can be integrated to yield the following temperature history during venting:

$$T = T_s + \frac{Q_T}{GAC_v}\ln\left(\frac{t_e}{t_e - t}\right) - \frac{V}{m_o}\frac{h_{fg}}{C_v v_{fg}}\left(\frac{t}{t_e - t}\right) \tag{29}$$

By setting the righthand side of Eq. 28 to zero, and solving for the turnaround time, τ, we obtain:

$$\tau = t_e - \left(\frac{Vh_{fg}}{Q_T v_{fg}}\right) \tag{30}$$

Again, this equation says that the time at turnaround is always less than the emptying time as long as latent-heat cooling is present. On substituting Eq. 30 into Eq. 29, the final equation for the maximum temperature during venting is obtained:

$$T_m - T_s = \frac{Q_T}{GAC_v}\left[\ln\left(\frac{m_o}{V}\frac{Q_T}{GA}\frac{v_{fg}}{h_{fg}}\right) - 1\right] + \frac{Vh_{fg}}{m_o C_v v_{fg}} \tag{31}$$

This is an expression implicit in relief vent rate such that for a given overpressure situation, the solution for GA is via iterative or graphical methods. But in the special case of no overpressure, Eq. 31 reduces to the correct limit:

$$A_o = \frac{Q_T m_o v_{fg}}{GVh_{fg}} \tag{32}$$

which is the same result as the runaway reaction case, Eq. 21, by noting that $Q_T = m_o q$ and $v = V/m_o$. This result, presented in a slightly different form by Forrest (1985), has found application in the treatment of fire exposure of storage vessels.

All-Vapor and All-Liquid Venting with External Heating

In these two limiting cases the energy equation takes the form,

$$mC_v \frac{dT}{dt} = Q_T - GAv_i \frac{h_{fg}}{v_{fg}} \tag{33}$$

Here again $v_i = v_g$ for all-vapor venting and $v_i = v_f$ for all-liquid venting. However, one readily recognizes that the two terms on the righthand side are independent of the mass inventory. Hence any slight imbalance between these two terms would cause a monotonic increase or decrease in temperature. At first glance, this implies that there is no merit in allowing for overpressure. In particular, for the all-vapor venting case, one should design for no overpressure, with the vent area obtained by setting the righthand side of Eq. 33 to zero:

$$A_o = \frac{Q_T v_{fg}}{Gv_g h_{fg}} \tag{34}$$

But for the all-liquid venting case, the pressure and temperature will eventually turn around when the vessel empties itself. The energy equation upon integration yields the following temperature history during venting:

$$T = T_s + \left(\frac{Q_T}{GAC_v} - \frac{v_f h_{fg}}{C_v v_{fg}}\right)\ln\left(\frac{t_e}{t_e - t}\right) \tag{35}$$

In order to avoid mathematical difficulty when t equals t_e, i.e., at complete mass depletion, we assume that the temperature turnaround occurs at 10% of the initial inventory:

$$\frac{m}{m_o} = \frac{t_e - \tau}{t_e} = 0.1 \quad \text{(turnaround criterion)}$$

[Note: $\ln(t_e/(t_e - \tau)) = \ln(m_o/m) = \ln(1/0.1) = 2.303$. Selection of other m/m_o values of close to zero, except zero of course, does not affect the numerical constant appreciably.]

Using this turnaround criterion, Eq. 35 yields the following vent rate

$$W = GA = \frac{Q_T}{\left[v_f \frac{h_{fg}}{v_{fg}} + \frac{C_v \Delta T}{2.303}\right]} \tag{36}$$

For the case of no overpressure, this equation reduces to the correct limit

$$A_o = \frac{Q_T v_{fg}}{Gv_f h_{fg}} \tag{37}$$

Discharge Flow Evaluation

In the above development we have obtained the required relief vent rate equations for the various situations of interest. The remaining task is one of selecting an appropriate mass flux G such that the ultimate vent area can be evaluated. In order to limit the scope, the present discussion is restricted to frictionless adiabatic flow characteristic of nozzles and short vent lines ($L/D < 50$; for complex configuration see Huff, 1985). Furthermore, we can assume quasi-steady state behavior and use the Bernoulli equation to provide an approximate description for the flow process between surfaces 1 and 2, Figure 2:

$$\frac{1}{2}(Gv_2)^2 + \int_1^2 v dP = 0 \tag{38}$$

Various critical flow models have been developed, starting with this equation, to account for at least two additional degrees of freedom in two-phase flows; namely, nonequilibrium effects and flow regime (phase slip) effects. Consider the case of a two-phase discharge of styrene in a frictionless vent line. Figure 3 depicts the mass flux as a function of upstream stagnation void fraction for the following discharge models:

HEM: Homogeneous equilibrium model (Starkman et al., 1964)

SEM: Slip equilibrium model (Moody, 1965)

HFM: Homogeneous nonequilibrium model (Henry and Fauske, 1971)

ERM: Equilibrium rate model (Fauske, 1985)

As shown, the homogeneous equilibrium model (equal velocity and temperature in both phases undergoing isentropic expansion) yields the lowest flow rates over the entire two-phase region and thus is conservative for ERS design. Recent studies reveal that this HEM agrees quite well with the available data for flow passage typical of a relief vent line. Based on published water critical flow data, Moody (1975) has shown that for pipes longer than 10 cm the equilibrium condition is closely approached, while for pipes approaching zero length the flow can be approximated by the nonflashing orifice equation. (For the

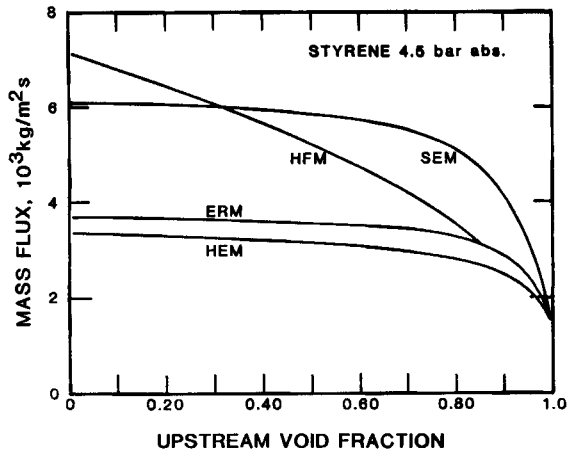

Figure 3. Critical flow rate for styrene as a function of inlet void fraction.

styrene example in Figure 3, this equation would yield a Bernoulli mass flux of about 15,000 kg/m^{2}s, certainly an overestimation of the flow in a practical vent line.) Furthermore, Moody showed that the maximum discharge rate data from vessels were adequately predicted by the homogeneous equilibrium model based on vessel stagnation conditions. At the same time a slip flow model was found to predict the equilibrium discharge rate in terms of local conditions at the nozzle throat or pipe exit. Thus, it appears that homogeneous choking normally occurs at the nozzle entrance and choking again occurs in the slip flow regime at the exit (Lahey and Moody, 1977). This relaxation length of 10 cm was shown by Fauske (1985) to hold true also for Freon-11 and Freon-12. In summary, the employment of the homogeneous equilibrium model in the relief discharge calculation is in fact a best-estimate evaluation and will not lead to overly conservative results.

Previously, the HEM has been rather time-consuming to use, requiring extensive saturated thermodynamic properties. Recently however, Leung (1986) has proposed a generalized correlation for this model with the scaling parameter ω given entirely in terms of known stagnation properties

$$\omega = \frac{x v_{fg}}{v} + \frac{C_p T P}{v}\left(\frac{v_{fg}}{h_{fg}}\right)^2 \tag{39}$$

In equation form, the generalized correlation gives the following normalized mass flux $G/\sqrt{P/v}$:

For $\omega \geq 4.0$ (low-quality region)

$$G/\sqrt{P/v} = [0.6055 + 0.1356(\ln \omega) - 0.0131(\ln \omega)^2]/\omega^{0.5} \tag{40a}$$

and for $\omega < 4.0$ (high-quality region)

$$G/\sqrt{P/v} = 0.66/\omega^{0.39} \tag{40b}$$

This greatly simplifies the discharge critical flow calculation and is applicable over the entire two-phase region. Furthermore, in the all-liquid inlet condition, the correlation may to a good approximation be replaced by

$$G \simeq 0.9\frac{h_{fg}}{v_{fg}}\left(\frac{1}{C_p T}\right)^{0.5} = 0.9G_L \tag{41}$$

where G_L is called the limiting flow by Grolmes and Leung (1984) and is also known as the approximate form for the equilibrium rate model by Fauske (1985). In most instances, Eq. 41 is also applicable to the homogeneous-vessel venting situation since the flow has a rather weak dependence on the upstream void fraction, as shown in Figure 3. On the other hand, in the all-vapor inlet condition, the present correlation does not necessarily give the same answer as the ideal gas formula (Bird et al., Eq. 15.5-42). This discrepancy is expected since a real vapor does not always behave as an ideal gas, particularly at the saturated region (Van Wylen and Sonntag, 1965). In applying this choked-flow correlation, one should also check for back-pressure effect (subcritical flow) particularly for high-quality flow situations; see Leung (1986) for critical pressure ratio correlation.

Styrene Polymerization Example

The first example is taken from Huff's (1982) paper which considers a tank of styrene monomer undergoing adiabatic polymerization after being heated inadvertently to 70°C. This tank has a maximum allowable working pressure (MAWP) of 5 bar absolute. The parameters are repeated here:

$V = 13.16\,\text{m}^3\,(3{,}500\,\text{gal})$

$m_o = 9{,}500\,\text{kg}$

$P_s = 4.5\,\text{bar abs.}$

$T_s = 209.4°\text{C} = 482.5\,\text{K}$

$(dT/dt)_s = 29.6°\text{C/min} = 0.493\,\text{K/s}\,(\text{sealed system})$

$P_m = 5.4\,\text{bar abs.}\,(\text{assuming } 10\%\,\text{above MAWP})$

$T_m = 219.5°\text{C} = 492.7\,\text{K}$

$(dT/dt)_m = 39.7°\text{C/min} = 0.662\,\text{K/s}$

Huff indicated that the above parameters were obtained from experimental data (using CSI-ARC device) recalculated to a ϕ factor of unity. The ϕ factor (also known as thermal inertia) according to Townsend and Tou (1980) is simply the ratio of the combined thermal capacity of the reacting sample and the sample container to that of the sample alone. Thus a ϕ factor of unity implies that the reacting sample is truly adiabatic. The following property data are taken from Huff's (1982) paper.

	4.5 Bar Set	5.4 Bar Peak
v_f, m^3/kg	0.001388	0.001414
v_g, m^3/kg; ideal gas assumed	0.08553	0.07278
C_p, kJ/kg · K	2.470	2.514
h_{fg}, kJ/kg	310.6	302.3

Based on two-phase homogeneous-vessel venting, the step-by-

step calculation proceeds as follow:

$$\Delta T = T_m - T_s = 10.2 \text{ K}$$

$$q = \frac{1}{2} C_v \left[\left(\frac{dT}{dt}\right)_s + \left(\frac{dT}{dt}\right)_m\right]$$

$$= 1.426 \text{ kJ/s} \cdot \text{kg (here } C_v \simeq C_p \text{ assumed)}$$

From Eq. 20

$$W = GA = \frac{(9{,}500)(1{,}426)}{\left\{\left(\frac{13.16}{9{,}500} \cdot \frac{310{,}600}{0.08414}\right)^{1/2} + [(2{,}470)(10.2)]^{1/2}\right\}^2}$$

$$= 256 \text{ kg/s}$$

In the above calculation, property parameters were evaluated at the set pressure only (using average values does not change this result significantly). According to Eqs. 14c and 18b, the emptying time and turnaround time are, respectively:

$$t_e = 9{,}500/256 = 37.1 \text{ s}$$

$$\tau = 37.1 - \left(\frac{13.16}{9{,}500} \cdot \frac{310{,}600}{0.08414} \cdot \frac{37.1}{1{,}426}\right)^{1/2}$$

$$= 37.1 - 11.5 \text{ s} = 25.6 \text{ s}$$

For comparison, Huff's (1982) method yields the following:

Case A: not accounting for vaporization time credit (i.e., $\Delta t_v = 0$)

$$\tau = \Delta t_p = 16.8 \text{ s}$$

$$W = 359 \text{ kg/s}$$

Case B: accounting for vaporization time credit

$$\Delta t_v = 7.6 \text{ s (trial-and-error solution)}$$

$$\tau = \Delta t_p + \Delta t_v = 24.4 \text{ s}$$

$$W = 267 \text{ kg/s}$$

The current method is hence in good agreement with Huff's more complete method (case B) but is simpler to apply without requiring trial-and-error solution.

Using the more traditional vapor-venting model, the no-overpressure case as given by Eq. 27 is

$$W = GA = \frac{(9{,}500)(1{,}219)(0.08414)}{(310{,}600)(0.08553)} = 37 \text{ kg/s}$$

Hence, the relief rate requirement is seven times less for all-vapor venting. Using the discharge flow equations mentioned earlier, we can compare the actual vent area for an ideal nozzle geometry:

Two-phase critical mass flux as given by the appropriate formula, Eq. 41,

$$G \simeq 0.9 \frac{310{,}600}{0.08414}\left[\frac{1}{(2{,}470)(482.5)}\right]^{1/2} = 3{,}040 \text{ kg/m}^2\text{s}$$

(Note: Eq. 40a yields nearly identical results, 3,090 kg/m^2 s.)

$$A = W/G = 256/3{,}040 = 0.084 \text{ m}^2$$

$$D = 0.327 \text{ m} \quad \text{(homogeneous-vessel venting)}$$

All-vapor critical mass flux as given by Eq. 40b

$$\omega = 1.4$$

$$G = \left(\frac{0.66}{\omega^{0.39}}\right)\left(\frac{P}{v_g}\right)^{1/2} = \left(\frac{0.66}{1.4^{0.39}}\right)\left(\frac{450{,}000}{0.08553}\right)^{1/2} = 1{,}310 \text{ kg/m}^2\text{s}$$

[Using the ideal gas formula with molecular weight of 104.15 and specific heat ratio of 1.05 yields 1,420 kg/m^2 s, which is 8% higher. However, the discrepancy is actually smaller due to the fact that real-gas specific volume (0.0782 m^3/kg from Redlich-Kwong EOS) is supposed to be used in this correlation. Such a calculation would yield a G of 1,370 kg/m^2 s.]

$$A = 37/1{,}310 = 0.026 \text{ m}^2$$

$$D = 0.189 \text{ m (all-vapor venting)}$$

The results obtained for this example case are summarized in Table 1 for the various design approaches. For both the Huff and Boyle methods, HEM critical flow rates are used instead of the discharge models suggested in their original papers. For the Fauske method using Eq. 3, the flow model is based on the ERM, which normally yields about 10% higher flow than the HEM. Table 1 illustrates that Boyle's emptying time criterion is most conservative, yielding the largest vent size. Huff's method accounting for vaporization time (case B) and the current approach give nearly identical results, with the smallest relief

Table 1. Comparison of Various Design Approaches

Method	Required Vent Rate W, kg/s	Discharge Mass Flux G, kg/m^2 · s	Ideal Nozzle Diameter D, m
Eq. 20	256	3,040	0.327
Huff			
Case A	359	3,360*	0.369
Case B	267	3,360	0.318
Boyle	566	3,040**	0.487
Fauske			
Eq. 3	459	3,560†	0.405
Nomograph	—	—	0.397
Vapor venting	37	1,310	0.189

*Based on HEM at peak pressure; original paper used HFM, which gave 4,490 kg/m^2 · s.
**Based on HEM at set pressure; original paper used nonflashing discharge flow.
†Based on ERM formula as given by $G = h_{fg}/v_{fg}\,(1/C_pT)^{0.5}$

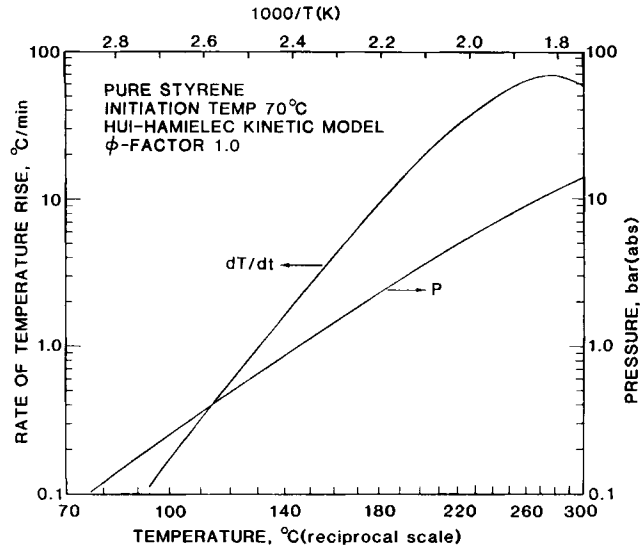

Figure 4. Self-heat rate and pressure-temperature data for styrene polymerization example.

requirement among two-phase venting results. Fauske's methods and Huff's other method (case A) lead to intermediate vent sizes. Finally, the all-vapor venting case yields the smallest vent size but this is considered nonconservative. If this size were employed, a much higher peak pressure would result since this particular system is known to yield two-phase discharge. Again, Eq. 20 can be used to estimate this peak pressure, as will be demonstrated later.

Another necessary and revealing comparison is between the current analytical approach and detailed computer simulations. Huff (1984b) reexamined the same styrene polymerization problem using computer simulation. Instead of utilizing the same set of experimental data as presented earlier, he employed the third-order kinetic model of Hui and Hamielec (1972) for styrene polymerization, as well as the Flory-Huggins correction for styrene partial pressure over polymer solution (Hildebrand and Scott, 1950). These equations and other physical property data were summarized in the appendix of Huff's (1982) paper. Self-heat rate data and P-T data are generated for a sealed adiabatic system as shown in Figure 4. We will now illustrate how these data together with the equations derived earlier can be used to predict the vessel behavior during relief. In Huff's simulation, a nonequilibrium discharge flow model was used. For consistency, the simulation was repeated for this study using the DIERS computer code (Grolmes and Leung, 1985) with the HEM discharge flow. Great care was exercised to ensure that this code reproduced the results shown in Figure 4 for a sealed system. Figure 5 illustrates the mass inventory, temperature, and pressure histories for a 5.4 bar peak pressure based on homogeneous-vessel venting with a 0.269 m nozzle diameter. The comparison is based on the same mass depletion rate as the computer simulation which is 202 kg/s. According to Figure 4, we obtain

	Set Condition	Peak Condition
P, bar abs.	4.54	5.4
T, K	488	499
dT/dt, °C/min	28	36

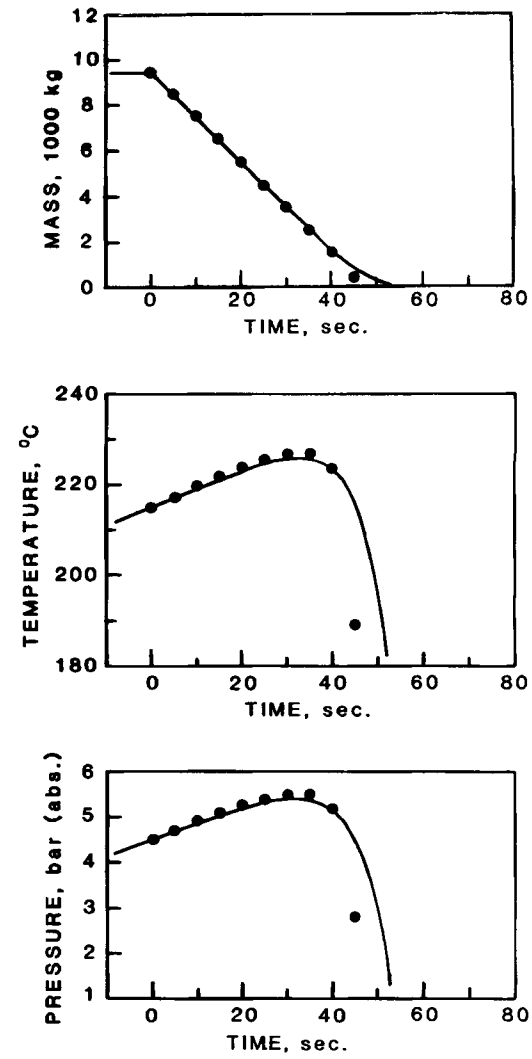

Figure 5. Comparison of predicted temperature and pressure histories (●●●●) with computer simulation (——) for styrene polymerization example.

Hence the average heat release rate q is 1,310 J/kg · s according to Eq. 22. The emptying time t_e as given by Eq. 14c is 47 s. The turnaround time τ is calculated to be 33 s using Eq. 18b; this is in excellent agreement with the simulation, as shown in Figure 5. Now the temperature history can be obtained from Eq. 17b in a straightforward manner. The corresponding pressure is simply based on a two-constant Antoine equation of the form

$$\ln P = a + \frac{b}{T} \tag{42}$$

where a and b are to be determined from Figure 5 using two representative points. The resulting temperature and pressure predictions, shown as circles in Figure 5, are in excellent agreement with the simulation. The faster fall-off in the temperature and pressure at 40 s occurs well past the turnaround time and hence is of no significance in the prediction of peak pressures during relief.

Phenolic Reaction Example

This example is taken from Booth et al. (1980) and the British Plastics Federation report (1980):

$V = 4.54\ m^3$
m_o = 3,628 kg (566 kg 38.3% formaldehyde aqueous solution, 2,150 kg phenol)
P_s = 2.07 bar abs.
P_m = 2.3 bar abs.

The second-order kinetic rate constant as given in their report is of the form:

$$k = 2.384 \times 10^{13} \exp\left[-\frac{12{,}386}{T}\right] (\text{kmol/kg})^{-1} \cdot \text{s}^{-1},$$

which implies an activation energy of 24.6 kcal/mol. The thermophysical values are taken to be independent of composition and temperature, and system pressure is computed as that of saturated water. The calculated self-heat rate and pressure data for a sealed system are shown in Figure 6; they are in agreement with the tabulated computer output of Appendix V of the British Plastics Federation report prior to venting. Figure 7 illustrates the inventory, temperature, and pressure histories for the homogeneous-vessel venting case with a 0.3 m vent diameter based on their own computer program. According to Figure 7, we obtain

	Set Condition	Peak Condition
P, bar abs.	2.07	2.21
T, K	394.4	396.7
dT/dt, °C/min	15	20

Using a specific heat value of 2,900 J/kg · K, the average heat release is 846 J/kg · s according to Eq. 22. Again, based on the same vent rate history (W = 150 kg/s), the turnaround time is calculated to be 14.9 s (h_{fg} = 2,502 kJ/kg, v_{fg} = 0.873 m³/kg, from the British Plastics Federation report). This is in excellent agreement with the program calculation. Both temperature and pressure are predicted in a fashion similar to the previous case, and as shown in Figure 7 by the solid circles, they are in close agreement with the British Plastics Federation study.

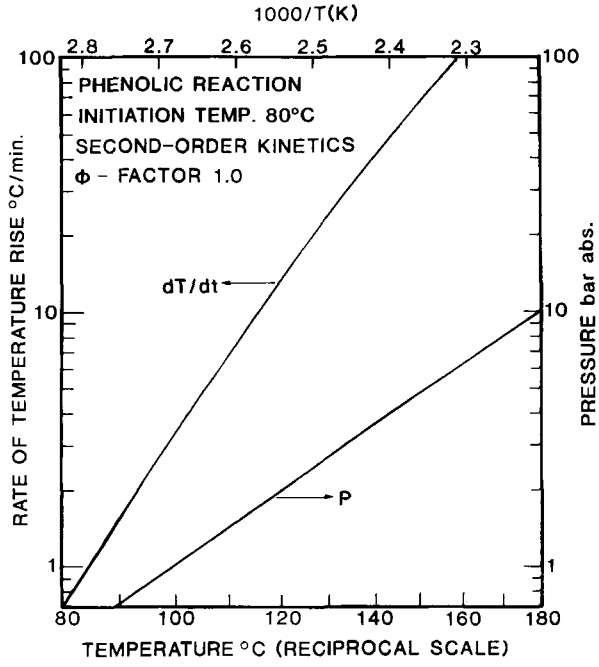

Figure 6. Self-heat rate and pressure-temperature data for phenolic reaction example.

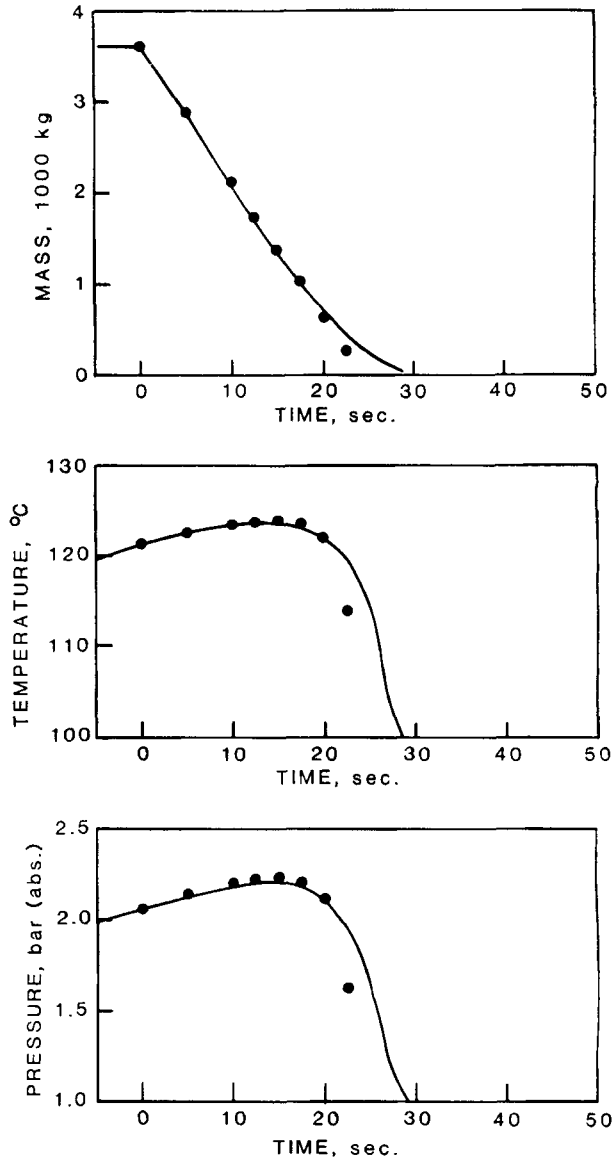

Figure 7. Comparison of predicted temperature and pressure histories (●●●●) with the British Plastic Federation study (——) for phenolic reaction example.

Vent Area Prediction Comparison

For homogeneous-vessel venting, Figure 8 depicts how the vent area varies with overpressure for the styrene example problem (using the Hui-Hamielec kinetic model). The analytical vent area predictions based on Eq. 20 are in good agreement with the computer simulation results over a wide range of overpressure. The slight discrepancy can be attributed to the mass

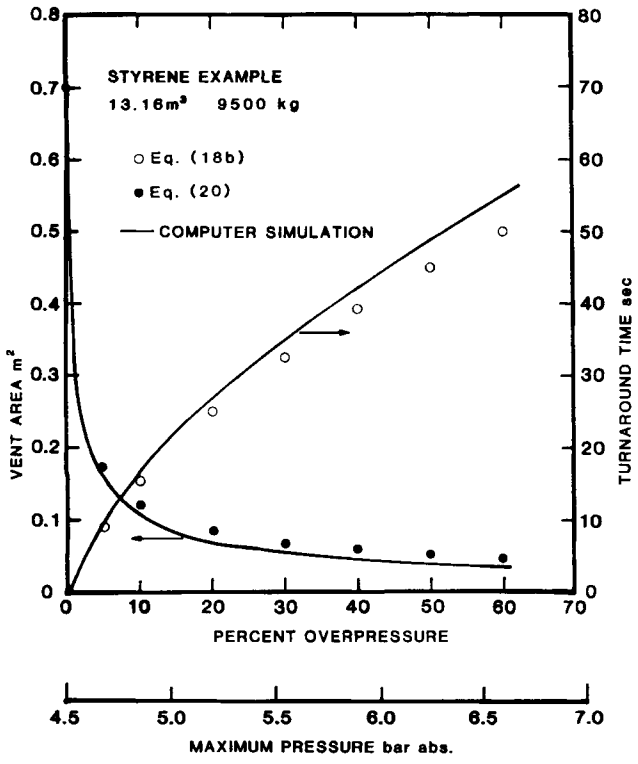

Figure 8. Vent area and turnaround time v. overpressure for styrene polymerization example.

flux estimations. The analytical prediction based on Eq. 41 and ideal gas vapor specific volume yields 3,040 kg/m^2 · s. The computer simulation, on the other hand, accounts for the compressibility effect in the vapor phase and yields a slightly higher flow of 3,400 kg/m^2 · s. If the real-gas specific volume of 0.0782 m^3/kg were used in Eq. 41, the flow would have been 3,350 kg/m^2 · s. A key observation, however, is the fact that a drastic reduction in vent area is obtained with a slight overpressure; this phenomenon has been noted earlier (Booth et al., 1980). Here the percent overpressure is defined conventionally in terms of gage set pressure as

$$\% \text{ overpressure} = \left(\frac{P_m(\text{bar g})}{P_s(\text{bar g})} - 1\right)100 \tag{43}$$

Thus, allowing for 10% overpressure in this case, the vent area is about six times smaller than the no-overpressure case. The reduction in area is a direct result of mass depletion in the reactor by venting. At the time of temperature turnaround, the total energy release term and the energy removal term on the right-hand side of Eq. 13 are equal, i.e.,

$$mq = GA\frac{V}{m}\frac{h_{fg}}{v_{fg}} \tag{44}$$

Thus the mass depletion contributes to reduction in vent area via two ways: (1) a decrease in total energy release, and (2) an increase in volumetric discharge at a higher two-phase specific volume which then leads to an increase in the energy removal rate via latent heat of vaporization. For the no-overpressure case, the turnaround time is 0 s; the relief requirement has to handle the energy release for the whole batch. But for the 10% overpressure case, the turnaround time is 15.3 s, as shown in Figure 8, and at this moment only 40% of the initial batch remains. Hence one readily obtains a sixfold [$(1/0.4)^2 \simeq 6$ according to Eq. 44] reduction in vent area.

Figure 8 also illustrates another important aspect of homogeneous-vessel venting: at higher overpressure the relative reduction in vent area becomes increasingly smaller. In fact, it is not recommended to design the relief system for such high overpressures even though the calculated maximum pressure may be less than or equal to the MAWP of the vessel. This is because a slight reduction in area can bring about a drastic increase in peak pressure reached. This portion of the curve is in essence operating on Boyle's emptying time concept with most of the energy release being stored as sensible heat in the batch. Due to the Arrhenius behavior typical of most reactions, this speeds up the reaction rate in an exponential fashion. The ultimate turnaround in pressure is due principally to the emptying of the reactor. This is obvious by considering Eq. 20 in the limit that the sensible heat accumulation term $C_v\Delta T$ is more pronounced than the evaporative cooling term vh_{fg}/v_{fg}, and the resulting equation approaches

$$A \rightarrow \frac{m_o q}{GC_v\Delta T} = \frac{m_o}{G\Delta t_p} \tag{45}$$

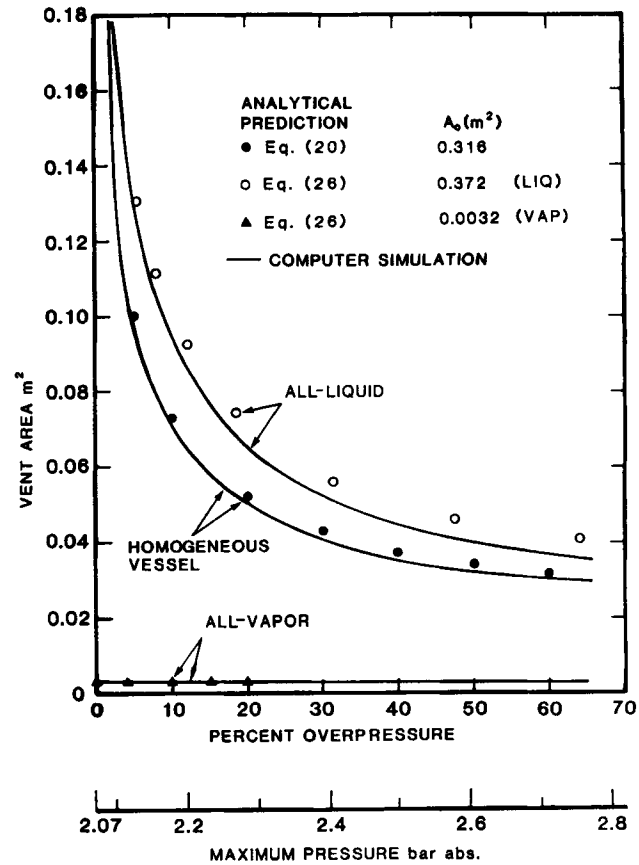

Figure 9. Vent area for three modes of venting v. overpressure for phenolic reaction example.

which is Boyle's formula. In summary, allowing for overpressure is both beneficial and permissible, and the amount of overpressure can best be guided by the knee of the curve, as shown in Figure 8, and in some cases by the MAWP of the vessel.

For the phenolic reaction example, all three venting modes are compared in Figure 9. The analytical predictions based on Eq. 20 for homogeneous-vessel venting and on Eq. 26 for all-vapor venting or for all-liquid venting, are in good agreement with the computer simulation results. The mass flux estimation likewise is based on Eq. 40a or Eq. 41 for the all-liquid and homogeneous-vessel venting cases, and on Eq. 40b for the all-vapor venting case. As expected, the all-liquid venting results are quite similar to the homogeneous-vessel venting behavior, both showing again the reduction in vent area with overpressure. The vent area corresponding to all-vapor venting is drastically smaller than all-liquid and two-phase discharge. Even though Eq. 26 yields the relationship between overpressure and vent area, it predicts little reduction in area with overpressure. This stems from the fact that in all-vapor venting no significant mass is lost, while the total energy release increases due to higher reaction rate with higher overpressure. Thus in practice there is little gain in allowing for overpressure in the case of all-vapor venting (Huff, 1982).

In the final example, we consider a LPG storage tank subjected to external fire without undergoing any chemical reaction. The problem is specified as follows:

$M_w = 44$ (propane)

$V = 100\ \text{m}^3$ (spherical)

$m_o = 50{,}700$ kg

$Q_T = 3{,}126$ kJ/s (based on 30 kW/m^2 surface heat flux)

$P_s = 4.5$ bar abs. (no pad)

$T_s = 271.5$ K

$h_{fg} = 3.74 \times 10^5$ J/kg

$v_{fg} = 0.1015\ \text{m}^3/\text{kg}$

The analytical predictions based on Eqs. 31, 36, and 34 for homogeneous-vessel venting, all-liquid venting, and all-vapor venting, respectively, are shown in Figure 10 to be in good agreement with the computer simulation results. Similar to the runaway reaction considered earlier, there is some reduction in vent area with overpressure for the homogeneous-vessel case although the relative reduction is less drastic here. Since the total energy input Q_T is treated as constant, the main cause for this vent area reduction is via increased two-phase specific volume in the discharge flow as a result of mass outage during venting. As for all-liquid venting, this reduction in area with overpressure is even less pronounced, as expected. In this situation the turnaround in pressure is due to emptying out the vessel content, and indeed this is assumed in the derivation of Eq. 36.

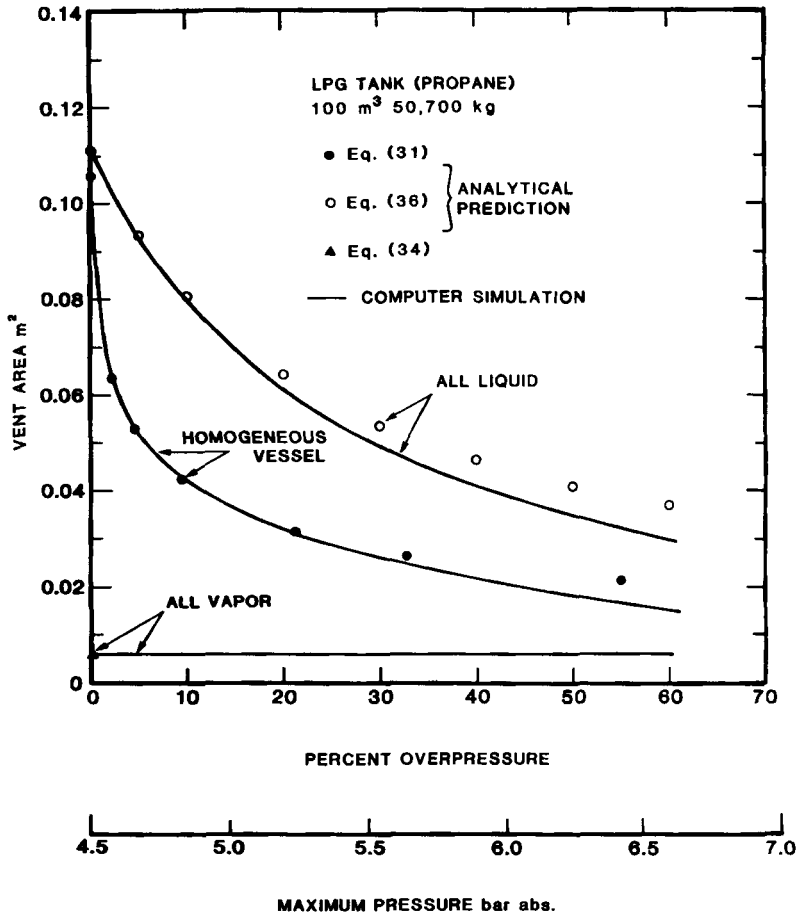

Figure 10. Vent area for three modes of venting v. overpressure for LPG storage vessel example.

Discussion and Limitation

Vent sizing equations presented in this paper also allow quick assessment of the effect on vent size due to changes or uncertainties in input parameters. Key parameters are identified as follows:

1. V, m_o
2. C_p, C_v (liquid)
3. h_{fg}, v_{fg}
4. P-T data
5. dT/dt v. T (sealed system)

Since specific heat at constant volume C_v is not commonly available, specific heat at constant pressure C_p can be used instead and the difference is small ($C_p = C_v$ for incompressible fluid). In the examples discussed in this paper, C_p values were used throughout. Because C_p values are always larger than C_v values (as discussed in most thermodynamic textbooks), this would only lead to slightly more conservative results. This can be seen from Eq. 20 in which the energy release rate q in the numerator is proportional to C_p, while the effect of C_p present in the denominator is somewhat lessened by the additive term. At zero overpressure, Eq. 20 says that the vent area is proportional to $C_p^{3/2}$, while at higher overpressure the proportionality becomes half-power. Hence for typical design at intermediate overpressure, the vent area is roughly proportional to the C_p value.

Another approximation can be made regarding h_{fg} and v_{fg} values, which always appear in the ratio h_{fg}/v_{fg}. Invoking the Clapeyron relation, this group can be replaced by

$$\frac{h_{fg}}{v_{fg}} = T\frac{dP}{dT} \tag{46}$$

which holds true for single-component fluids and is generally a good approximation for multicomponent mixtures where composition change is minimal (Dodge, 1944; Stein, 1979). This is immensely useful since available P-T data can be utilized.

Finally, the self-heat rate in runaway reactions can best be obtained experimentally in an apparatus that offers little heat capacity of its own (Fauske and Leung, 1985). The alternative would require detailed reaction kinetic modeling, which is both time-consuming and expensive.

In this development, partial liquid-vapor disengagement has not been considered. In a churn-turbulent regime (Wallis, 1969), the two-phase quality entering the relief vent line can be substantially higher than the vessel average (Grolmes and Fauske, 1984). This results in a higher volumetric flow and a smaller required vent size than that of homogeneous-vessel treatment. Since this kind of flow regime cannot be predicted *a priori* without actual flow-regime characterization data, it is prudent to assume homogeneous-vessel venting in order to assure a safe ERS design (Fauske, 1984b).

The present treatment has been limited to a liquid phase system; pure gaseous phase and solid phase systems are not covered in this paper. For reactions that generate gaseous products—so-called gassy reactions—the runaway exotherm may or may not be tempered by evaporative cooling. Examples have been given by Huff (1984a), but treatment of such systems is far more complex and should receive further investigation.

Finally, it should be noted that the present treatment would break down as the thermodynamic critical region is approached. Fortunately, for most of the exothermic reacting systems the relief set pressures are far removed from this regime.

Acknowledgment

Most of this work was performed under a R&D contract from the Design Institute for Emergency Relief Systems (DIERS) of AIChE. Many helpful comments from H. G. Fisher (Union Carbide Corporation), H. S. Forrest (FMC Corporation), and L. J. Manda (Monsanto Corporation) are acknowledged. Constructive criticism of the original manuscript by J. E. Huff (Dow Chemical Company) is also appreciated.

Notation

A = ideal vent area
A_o = zero overpressure vent area
C_p = liquid specific heat at constant pressure
C_v = liquid specific heat at constant volume
C_{pj} = specific heat at constant pressure of jth phase
C_{vj} = specific heat at constant volume of jth phase
D = ideal vent diameter
e_1 = specific energy entering vent line
G = mass velocity or flux, mass flow rate per unit area
G_L = limiting flow corresponding to ERM model, Eq. 41
h = specific enthalpy
h_{fg} = latent heat of vaporization
k = reaction rate constant
L = pipe length
m = instantaneous mass in vessel
m_o = initial mass in vessel
M_w = molecular weight
P = system pressure, absolute unless specified
q = heat release rate per unit mass
Q = total heat input or release rate
R = gas law constant
t = time
t_e = emptying time, Eq. 14c
T = system temperature
u = specific internal energy
v = specific volume
V = volume of vessel
W = relief mass flow rate or vent rate
x = quality or mass fraction of vapor

Greek letters

β = parameter, Eq. 5
γ = specific heat ratio
ρ = density
ΔP = overpressure, $P_m - P_s$
ΔT = temperature rise above set, $T_m - T_s$, corresponding to ΔP
Δt_p = time for pressure to rise from set point to specified level in sealed system
Δt_v = vaporization time, Figure 1
τ = turnaround time in pressure (p) or temperature (t)
ω = critical flow scaling parameter, Eq. 39

Subscripts

1 = location at vent line entry point, Figure 2
2 = location at vent line exit point, Figure 2
ext = external
f = liquid phase
g = gas (vapor) phase
fg = difference between gas (vapor) phase and liquid phase
i = ith phase
m = at peak pressure or temperature
o = initial
rxn = reaction
s = set point
T = total

Literature cited

Bird, R. B., W. E. Stewart, and E. N. Lightfoot, *Transport Phenomena*, Wiley New York (1960).

Booth, A. D., M. Karmarkar, K. Knight, and R. C. L. Potter, "Design of Emergency Venting System for Phenolic Resin Reactors. 1, 2," *Trans. Inst. Chem. Eng.*, **58**, 75 (1980).

Boyle, W. J., Jr., "Sizing Relief Area for Polymerization Reactors," *Chem. Eng. Prog.*, **63** (8), 61 (Aug., 1967).
British Plastics Federation, "Guidelines for the Safe Production of Phenolic Resins," Report by Thermosetting Materials Group (1980).
Diss, E., H. Karam, and C. Jones, "Practical Way to Size Safety Discs," *Chem. Eng.*, **68** (19), 187 (Sept. 18, 1961).
Dodge, B. F., *Chemical Engineering Thermodynamics*, McGraw-Hill, New York (1944).
Duxbury, H. A., "Relief System Sizing for Polymerization Reactors," *Chem. Eng.*, 31 (Jan., 1980).
Fauske, H. K., "Scale-up for Safety Relief of Runaway Reactions," *Plant/Operations Prog.*, **3** (1), 7 (Jan., 1984a).
———, "A Quick Approach to Reactor Vent Sizing," *Plant/Operations Prog.*, **3** (3), 145 (July, 1984b).
———, "Generalized Vent Sizing Nomogram for Runaway Chemical Reactions," *Plant/Operations Prog.*, **3** (4), 213 (Oct., 1984c).
———, "Flashing Flows—Some Practical Guidelines for Emergency Releases," *Plant/Operations Prog.*, **4** (3), 132 (July, 1985).
Fauske, H. K., and J. C. Leung, "New Experimental Technique for Characterizing Runaway Chemical Reactions," *Chem. Eng. Prog.*, **81** (8), 39 (Aug., 1985).
Forrest, H. S., "Emergency Relief Vent Sizing for Fire Exposure when Two-Phase Flow Must Be Considered," Paper No. 56e, *19th Loss Prevention Symp.*, AIChE Nat. Meet., Houston (Mar., 1985).
Grolmes, M. A., and H. K. Fauske, "An Evaluation of Incomplete Vapor Phase Separation in Freon-12 Top-Vented Depressurization Experiments," *Multiphase Flow Heat Transfer* **III**, A: *Fundamentals*, T. N. Veziroglu and A. E. Bergles, eds., Elsevier, Amsterdam (1984).
Grolmes, M. A., and J. C. Leung, "Scaling Considerations for Two-Phase Critical Flow," *Multiphase Flow and Heat Transfer* **III**, A: *Fundamentals*, T. N. Veziroglu and A. E. Bergles, eds., Elsevier, Amsterdam (1984).
———, "Code Method for Evaluating Integrated Relief Phenomena," *Chem. Eng. Prog.*, **81** (8), 47 (Aug., 1985).
Harmon, G. W., and H. A. Martin, "Sizing Rupture Discs for Vessels Contatining Monomers," Prepr. No. 58a, *67th Nat. Meet.* AIChE (Feb., 1970).
Henry, R. E., and H. K. Fauske, "The Two-Phase Critical Flow of One-Component Mixtures in Nozzles, Orifices, and Short Tubes," *J. Heat Trans., Trans. ASME*, **93**, 179 (1971).
Hildebrand, J. H., and R. L. Scott, *The Solubility of Nonelectrolytes*, Reinhold, New York (1950).
Huff, J. E., "Computer Simulation of Polymerizer Pressure Relief," *Chem. Engr. Prog., Loss Prevention Tech. Manual*, **7**, 45 (1973).
———, "A General Approach to the Sizing of Emergency Pressure Relief Systems," *Proc. 2nd Int. Symp. Loss Prevention Safety Promotion in Process Industries*, Heidelberg, (Sept., 1977); also "Supporting Derivations and Discussion for Paper: A General Approach to the Sizing of Emergency Pressure Relief Systems," supplement issued at symposium, Dechema, Frankfurt (1977).
———, "Emergency Venting Requirements," *Plant/Operations Prog.*, **1** (4), 211 (Oct., 1982).
———, "Emergency Venting Requirements for Gassy Reactions from Closed-System Tests," *Plant/Operations Prog.*, **3** (1), 50 (Jan., 1984a).
———, "Computer Simulation of Runaway Reaction Venting," *I. Chem. E., Symp. Ser.* No. 85, 109 (Apr., 1984b).
———, "Multiphase Flashing Flow in Pressure Relief Systems," *Plant/Operations Prog.*, **4** (4), 191 (Oct., 1985).
Hui, A. W., and A. E. Hamielec, "Thermal Polymerization of Styrene at High Conversions and Temperatures. An Experimental Study," *J. Appl. Polymer Sci.*, **16**, 749 (1972.)
Lahey, R. T., and F. J. Moody, *The Thermal-Hydraulics of a Boiling Water Nuclear Reactor*, Am. Nuclear Soc., Hinsdale, IL (1977).
Leung, J. C., "A Generalized Correlation for One-Component Homogeneous Equilibrium Flashing Choked Flow," to be published in the *AIChE J.* (1986).
Moody, F. J., "Maximum Flow Rate of a Single-Component, Two-Phase Mixture," *J. Heat Transfer, Trans. ASME*, **87**, 134 (1965).
———, "Maximum Discharge Rate of Liquid Vapor Mixtures from Vessels," *Nonequilibrium Two-Phase Flows, ASME Symp. Vol.*, Am. Soc. Mech. Eng. (1975).
Smith, J. M., *Chemical Engineering Kinetics*, 2nd Ed. McGraw-Hill, New York (1970).
Starkman, E. S., V. E. Shrock, K. F. Neusen, and D. J. Maneely, "Expansion of a Very Low-Quality Two-Phase Fluid Through a Convergent-Divergent Nozzle," *J. Basic Eng., Trans. ASME*, **68** (2), 247 (1964).
Stein, H. N., "Some Thermodynamic Relations for Binary Liquid-Gas Equilibria," *Boiling Phenomena*, S. van Stralen and R. Cole, eds., Hemisphere, McGraw-Hill, New York **2**, 535 (1979).
Townsend, D. I., and J. C. Tou, "Thermal Hazard Evaluation by an Accelerating Rate Calorimeter," *Thermochimica Acta*, **37**, 1 (1980).
Van Wylen, G. J., and R. E. Sonntag, *Fundamentals of Classical Thermodynamics*, Chapter 14, John Wiley, New York (1965).
Wallis, G. B., *One-Dimensional Two-Phase Flow*, McGraw-Hill, New York, (1969).

Manuscript received July 11, 1985, and revision received Feb. 21, 1986.